Flattening of Wavelength Characteristics of Reflected Dominant Guided Mode in Index-Modulation Type Periodic 3-D Optical waveguide *

Michiko MOMODA**, Tokuo MIYAMOTO** and Kiyotoshi YASUMOTO***

Wavelength characteristics of reflected dominant guided mode in index-modulation type periodic 3-D optical waveguide usually show asymmetry, because the reflected power of radiation field increases as the wavelength becomes shorter than the Bragg wavelength. In this report, it is confirmed that, in the fiber Bragg grating and the embedded periodic waveguide with rectangular cross-section, such a radiation field can be suppressed remarkably by making the cladding or the substrate part periodic structure similarly as the guided part, and the wavelength characteristics approach symmetry and are flattened.

Key Words: Numerical Analysis, 3-D Periodic Waveguide, Wavelength Characteristics

1. Introduction

Optical fiber grating and various types of three-dimensional thin-film periodic optical waveguides have been playing important roles as a filter and other devices in optical IC. However wavelength characteristics of main lobe of reflected dominant guided mode in periodic waveguide usually show asymmetry, because the reflected power of radiation field increases as the wavelength becomes shorter than the Bragg wavelength[1]-[3]. The authors have confirmed that a lamellar grating type periodic embedded waveguide is very effective for the suppression of such a radiation field and the flattening of the wavelength characteristics of the main lobe[4],[5]. However, as for the index-modulation type periodic thin-film optical waveguide with air cover, the suppression of the reflected radiation field has been difficult[1]. In a fiber Bragg grating, suppression of the radiation field has been achieved by making also the cladding part periodic structure[6].

In this paper, using the Fourier series expansion method, the authors tried to suppress such a radiation field also in an index-modulation type periodic embedded optical waveguide with rectangular cross-section covered partly by air cover, applying the same idea as the case of fiber Bragg grating[6]. That is, by making also the substrate part periodic structure, it is confirmed that the radiation field can also be suppressed remarkably and the wavelength characteristics of the main lobe in reflected dominant guided mode can be flattened, even in the case where the cover is air[7],[8]. Then its numerical results are reported in detail.

2. Numerical method

Detail algorithm of the Fourier series expansion method are referred in the literatures [2] and [3]. For convenience, we consider the following normalized Maxwell equations

$$\nabla\times\mathbf{E}(x,y,z)=-j\mathbf{H}(x,y,z),$$
$$\nabla\times\mathbf{H}(x,y,z)=j\varepsilon(x,y)\mathbf{E}(x,y,z), \qquad (1)$$

and obtain the electromagnetic field by solving Eq.(1)

* 平成18年7月31日受付
** Department of Electronics Engineering and Computer Science, Faculty of Engineering, Fukuoka University
*** Faculty of Information Science and Electrical Engineering, Kyushu University

using Fourier series expansion method with virtual periodic boundaries. The electromagnetic field components satisfying Eq.(1) can be expressed by the following complex double Fourier polynomials introducing virtual periods Λ_x and Λ_y:

$$E_i(x,y,z)=\sum_{m=-M}^{M}\sum_{n=-N}^{N}e^{i}_{m,n}(z)\exp(-jsmx)\exp(-jtny),$$
$$H_i(x,y,z)=\sum_{m=-M}^{M}\sum_{n=-N}^{N}h^{i}_{m,n}(z)\exp(-jsmx)\exp(-jtny),$$
$$i=x,y,z\quad s=2\pi/\Lambda_x,\quad t=2\pi/\Lambda_y. \tag{2}$$

Eq.(2) is substituted into Eq.(1), then the following matrix form of second order differential equation in z is derived:

$$d^2\mathbf{e}(z)/dz^2=-\mathbf{C}\mathbf{e}(z) \tag{3}$$

where the transverse Fourier coefficients $\{e^{i}_{m,n}(z)\}$ $(i=x,y)$ are expressed by column vectors $\mathbf{e}(z)$ of order 2K $(K=(2M+1)(2N+1))$, and $\mathbf{C}$ is composed, of K-th order diagonal matrices $[sm\delta_{mm'}\delta_{nn'}]$ and $[tn\delta_{mm'}\delta_{nn'}]$ and Fourier coefficient matrix of $\varepsilon(x,y)$. Eq.(3) is reduced to an eigenvalue problem of the coefficient matrix $\mathbf{C}$ of order 2K, then the eigenvalue κ_k^2 and the corresponding eigenvector $\mathbf{P}^e_k$(k=1,2,……, 2K) can be obtained readily by a standard subroutine. Using the solution $\mathbf{P}^e_k$ and the relation $\mathbf{e}(z)=\mathbf{P}^e\mathbf{a}(z)$ where $\mathbf{P}^e=[\mathbf{P}^e_1,\mathbf{P}^e_2,\cdots,\mathbf{P}^e_{2K}]$, Eq.(3) can be solved with regard to the new vector variable $\mathbf{a}(z)=[\mathbf{a}^+(z)\ \mathbf{a}^-(z)]^t$ of order 2K as follows:

$$\mathbf{f}(z)=\mathbf{P}\mathbf{U}(z-z_0)\mathbf{a}(z_0),$$
$$\mathbf{U}(\Delta z)=\begin{bmatrix}\mathbf{U}^+(\Delta z) & \mathbf{0}\\ \mathbf{0} & \mathbf{U}^-(\Delta z)\end{bmatrix},$$
$$\mathbf{U}^{\pm}(\Delta z)=[\exp\{\mp jk(\Delta z)\}\delta_{kk'}],$$
$$\mathbf{P}=\begin{bmatrix}\mathbf{P}^e & \mathbf{P}^e\\ \mathbf{P}^h & -\mathbf{P}^h\end{bmatrix},\ \mathbf{P}^h=[\kappa_k\delta_{kk'}]\mathbf{C}_1^{-1}\mathbf{P}^e. \tag{4}$$

Here superscripts $\pm$ indicate the propagation to $\pm$z-directions, respectively. $\mathbf{f}(z)=[\mathbf{e}(z)\ \mathbf{h}(z)]^t$ and vector $\mathbf{h}(z)$ on expansion coefficient $\{h^{i}_{m,n}(z)\}$ can be obtained from the solution $\mathbf{e}(z)$ by the relation of Maxwell equations.

Next, we consider the problem of connection between each region Ⅰ, Ⅱ within one period L in each figure. The boundary conditions on electro-magnetic fields satisfy $\mathbf{f}^{\mathrm{I}}(z_i)=\mathbf{f}^{\mathrm{II}}(z_i)(i=1,2)$ [2]. From these relations we derive

$$\mathbf{a}^{\mathrm{I}}(L)=\mathbf{F}_a\mathbf{a}^{\mathrm{I}}(0), \tag{5}$$
$$\mathbf{F}_a=\mathbf{U}^{\mathrm{I}}(\Delta z/2)(\mathbf{P}^{\mathrm{I}})^{-1}\mathbf{P}^{\mathrm{II}}\mathbf{U}^{\mathrm{II}}(\Delta z)(\mathbf{P}^{\mathrm{II}})^{-1}\mathbf{P}^{\mathrm{I}}\mathbf{U}^{\mathrm{I}}(\Delta z/2) \tag{6}$$

Here, $\mathbf{F}_a$ is the transfer matrix of the mode amplitude $\mathbf{a}^{\mathrm{I}}$ at one symmetric grating period L. Expressing the eigenvalue and eigenvector of matrix $\mathbf{F}_a$ as $\exp(-j\gamma_l L)$ and $[\mathbf{X}_{1,l}\ \ \mathbf{X}_{2,l}]^t$ $(l=1,2,\cdots 2K)$, respectively, following relations can be derived:

$$\mathbf{F}_a=\mathbf{X}\mathbf{V}(L)\mathbf{X}^{-1}, \tag{7}$$
$$\mathbf{X}=\begin{bmatrix}\mathbf{X}_1 & \mathbf{X}_2\\ \mathbf{X}_2 & \mathbf{X}_1\end{bmatrix},\ \mathbf{V}(L)=\begin{bmatrix}\mathbf{V}^+(L) & \mathbf{0}\\ \mathbf{0} & \mathbf{V}^-(L)\end{bmatrix},$$
$$\mathbf{X}_i=[\mathbf{X}_{i,1},\mathbf{X}_{i,2},\cdots,\mathbf{X}_{i,2K}],\ i=1,2,$$
$$\mathbf{V}^{\pm}(L)=[\exp(\mp j\gamma_l L)\delta_{ll'}]. \tag{8}$$

From Eqs.(5) and (7), and the relation $\mathbf{b}^{\mathrm{I}}(z)=\mathbf{X}^{-1}\mathbf{a}^{\mathrm{I}}(z)$, we obtain the relation $\mathbf{b}^{\mathrm{I}}(L)=\mathbf{V}(L)\mathbf{b}^{\mathrm{I}}(0)$. Here $\mathbf{b}^{\mathrm{I}}$ is amplitude vector of Floquet mode. In the case of grating with finite length consisting of N_g periods,

$$\mathbf{b}^{\mathrm{I}}(N_gL)=\mathbf{V}(N_gL)\mathbf{b}^{\mathrm{I}}(0) \tag{9}$$

is obtained. This relation can be rearranged in terms $\mathbf{a}^{\mathrm{I}}(z)$ as follows:

$$\begin{bmatrix}\mathbf{R}_{11} & -\mathbf{V}^+(N_gL)\mathbf{R}_{12}\\ \mathbf{V}^+(N_gL)\mathbf{R}_{21} & -\mathbf{R}_{22}\end{bmatrix}\begin{bmatrix}\mathbf{a}^{\mathrm{I}+}(N_gL)\\ \mathbf{a}^{\mathrm{I}-}(0)\end{bmatrix}$$
$$=\begin{bmatrix}\mathbf{V}^+(N_gL)\mathbf{R}_{11} & -\mathbf{R}_{12}\\ \mathbf{R}_{21} & -\mathbf{V}^+(N_gL)\mathbf{R}_{22}\end{bmatrix}\begin{bmatrix}\mathbf{a}^{\mathrm{I}+}(0)\\ \mathbf{a}^{\mathrm{I}-}(N_gL)\end{bmatrix} \tag{10}$$

where the 4 miner matrices of $\mathbf{X}^{-1}$ are expressed as $\mathbf{R}_{11}$, $\mathbf{R}_{12}$, $\mathbf{R}_{21}$ and $\mathbf{R}_{22}$, and the relation $\mathbf{b}^{\mathrm{I}-}(0)=\mathbf{V}^+(N_gL)\mathbf{b}^{\mathrm{I}-}(N_gL)$ is substituted in Eq.(9) in order to eliminate the term $\mathbf{V}^-(N_gL)$ which is a cause of the growing wave for the evanescent wave. We assumed that the dominant mode HE_{11} is incident at z=0 and that there is no reflection from $z>N_gL$. Then the initial conditions are expressed as

$$\mathbf{a}^{\mathrm{I}+}(0)=[1\ 0\ \cdots\ 0]^t,\quad \mathbf{a}^{\mathrm{I}-}(N_gL)=\mathbf{0}. \tag{11}$$

Substituting these conditions into Eq.(10), solutions $\mathbf{a}^{\mathrm{I}-}(0)$ and $\mathbf{a}^{\mathrm{I}+}(N_gL)$ are obtained. Then the reflected powers R_g, R_r and the transmitted powers T_g, T_r of the guided modes and radiation fields can be expressed, respectively, as

$$R_g=\sum_{k=1}^{K_1}|a_k^{I-}(0)|^2,\ R_r=\sum_{k=K_1+1}^{2K}|a_k^{I-}(0)|^2,$$

$$T_g=\sum_{k=1}^{K_3}|a_k^{I+}(N_gL)|^2,\ T_r=\sum_{k=K_3+1}^{2K}|a_k^{I+}(N_gL)|^2, \quad (12)$$

$$T_g+T_r+R_g+R_r=1. \quad (13)$$

Here K_1 is the number of guided mode. The eigenvectors are normalized in such a way that the total power of k-th mode carried in the z-direction is $|a_k|^2$.

3. Numerical results

In order to suppress the growing radiation field in the shorter wavelength region, first a fiber Bragg grating as shown in Fig.1(a) is chosen. In the numerical calculation, the wavelength characteristics of reflected powers R_{g1} of dominant guided mode and R_r of total radiation field are obtained for dominant mode incidence at z=0, using Fourier series expansion method [2],[3]. As shown in Fig.1(b), by making also the cladding part (n_c) periodic structure (n_{c1}, n_{c2}) similarly as the core grating, radiation field can be suppressed remarkably ($R_r\sim10^{-4}$) and the flat wavelength characteristics can be obtained [7],[8]. Here $n_{c2}/n_{c1}\sim n_{f2}/n_{f1}$ (see Fig.4).

This phenomena is caused by the fact that the magnitude of the field at cladding edge ($y=0, \Lambda_x$) becomes negligibly small, then the diffraction from the edge can be suppressed remarkably, comparing to the normal fiber grating in which the magnitude of electric field is large at the core edge as shown in Fig.1(a).

Next we apply this technique to the embedded periodic 3-D waveguide with air cover ($n_c=1.0$) as shown in Fig.2(a) in which radiation field in the shorter wavelength region is so large. Then refractive index n_s of the substrate part is also changed periodically (n_{s1}, n_{s2}), corresponding to the change of the refractive index of the periodic guiding part (n_{f1}, n_{f2}) as shown in Fig.2(b). The ratio of n_{s2}/n_{s1} is chosen so that $n_{s2}/n_{s1}\sim n_{f2}/n_{f1}$ according to the later investigation (in Fig.4). In this case too, it

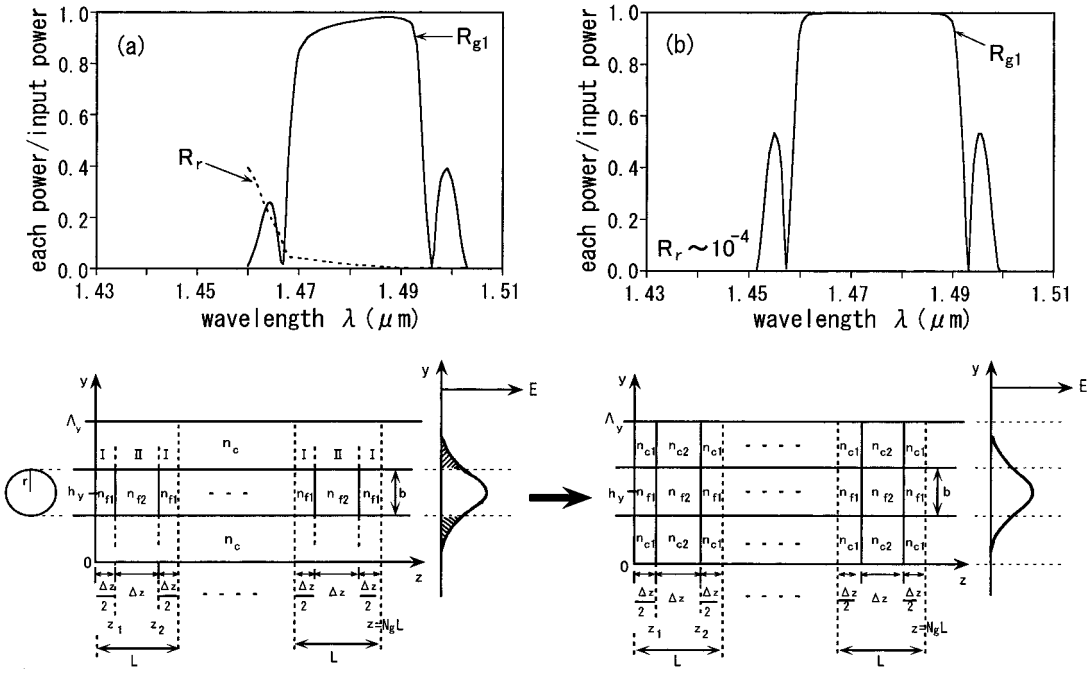

(a) normal fiber Bragg grating (b) improved fiber Bragg grating

Fig.1 Suppression of radiation field in the fiber Bragg grating
(r=1[μm], Δz=0.25[μm], $\Lambda_x=\Lambda_y=10\lambda$, $n_{f1}=1.55$, $n_{f2}=1.50$, $n_c=n_{c1}=1.45$, $n_{c2}=1.40$, $N_g=150$, M=N=10)

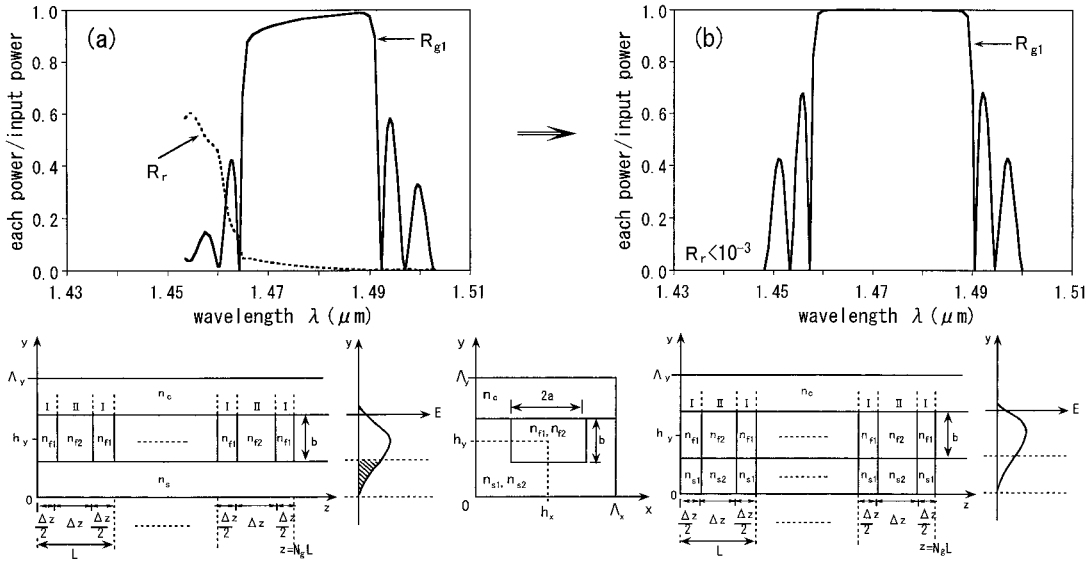

(a) normal embedded periodic waveguide　　(b) improved embedded periodic waveguide

Fig.2 Suppression of radiation field in the index-modulation type periodic waveguide with rectangular cross-section
($n_{f1}=1.55$, $n_{f2}=1.50$, $n_s=n_{s1}=1.45$, $n_{s2}=1.40$, $n_c=1.0$, $2a=3[\mu m]$, $b=1.5[\mu m]$, $\Delta z=0.25[\mu m]$, $L=0.5[\mu m]$, $N_g=200$, $\Lambda_x=\Lambda_y=10\lambda$, $M=N=10$)

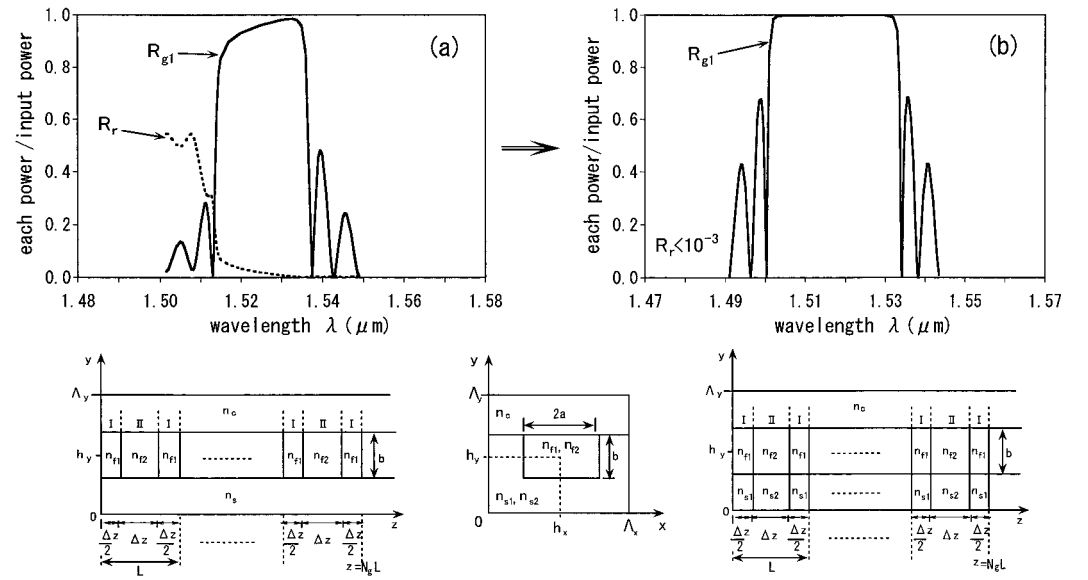

(a) normal embedded periodic waveguide　　(b) improved embedded periodic waveguide

Fig.3 Suppression of radiation field in the index-modulation type periodic waveguide with rectangular cross-section
($n_{f1}=3.5$, $n_{f2}=3.38$, $n_s=n_{s1}=3.27$, $n_{s2}=3.17$, $n_c=1.0$, $2a=1.6[\mu m]$, $b=0.8[\mu m]$, $\Delta z=0.114[\mu m]$, $L=0.228[\mu m]$, $N_g=200$, $\Lambda_x=\Lambda_y=10\lambda$, $M=N=10$)

is confirmed that the radiation field is suppressed remarkably (small than 10^{-3}), similarly as the case of fiber Bragg grating (Fig.1), and the wavelength characteristics is flattened. The edge part of the main lobe can be sharpened by increasing N_g. In Fig.3, the same investigation as the case of glass substrate (Fig.2) is achieved for the semi-conductor substrate. Similar characteristics are obtained, although the width of the main lobe of R_{g1} is narrower.

According to these results, it is confirmed that the suppression method [6] of the radiation field which is applied effectively for fiber Bragg grating is also effective to the case of index-modulation type periodic waveguide with rectangular cross-section where the cover part is air.

n_{s2}	R_{g1}	R_r
3.12	0.9945	0.00300
3.14	0.9966	0.00180
3.15	0.9974	0.00130
3.16	0.9981	0.00097
3.17	0.9985	0.00075
3.18	0.9985	0.00074
3.19	0.9981	0.00095
3.20	0.9972	0.00140
3.21	0.9955	0.00230
3.24	0.9830	0.00860
3.26	0.9610	0.01800
3.27	0.9380	0.02700

Table.1 Magnitude of R_{g1} and R_r at $\lambda=1.513[\mu m]$

Fig.4 shows the behavior of the wavelength characteristics of the main lobe of R_{g1} when n_{s2} is changed from 3.27 (normal periodic waveguide) to 3.12 (periodic substrate), in which $n_c=3.0$. It is confirmed that the magnitude of radiation field in the shorter wavelength decreases and the asymmetry of the wavelength characteristics in the main love is weakened as n_{s2} becomes small. When the ratio n_{s2}/n_{s1} approaches $n_{f2}/n_{f1}\sim0.97$, the asymmetry becomes smallest and flat wavelength characteristics can be obtained. However, it is noted that for smaller value than 3.16 asymmetry begins to increase again (see also Table 1).

Fig.5 shows the difference between the cases of $n_c=3.0$ covered by a semi-conductor layer and air cover ($n_c=1.0$). In the case of $n_c=3.0$, the field distribution of dominant guided mode penetrates to the cover part as shown the Fig.5, then the diffraction

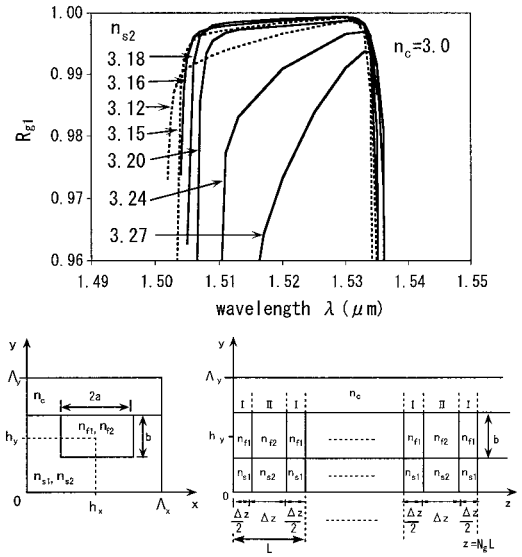

Fig.4 Wavelength characteristics of R_{g1} in index-modulation type periodic waveguide with $n_c=3.0$, when the refractive index n_{s2} is changed from 3.27 to 3.12 ($n_{f1}=3.5$, $n_{f2}=3.38$, $n_{s1}=3.27$, $n_{s2}=3.15\sim3.27$, $n_c=3.0$, $2a=1.6[\mu m]$, $b=0.8[\mu m]$, $\Delta z=0.114[\mu m]$, $L=0.228[\mu m]$, $N_g=200$, $\Lambda_x=\Lambda_y=10\lambda$, $M=N=10$)

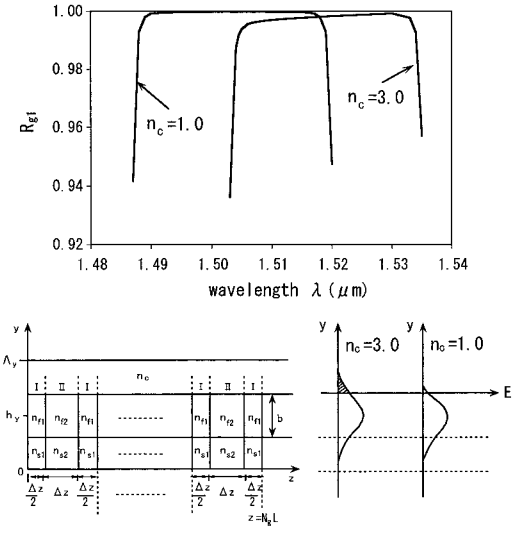

Fig.5 Wavelength characteristics of R_{g1} in improved index-modulation type periodic waveguide for the refractive indices of cover changed $n_c=1.0$ and $n_c=3.0$ ($n_{f1}=3.5$, $n_{f2}=3.38$, $n_{s1}=3.27$, $n_{s2}=3.15$, $n_c=3.0, 1.0$, $2a=1.6[\mu m]$, $b=0.8[\mu m]$, $\Delta z=0.114[\mu m]$, $L=0.228[\mu m]$, $N_g=200$, $\Lambda_x=\Lambda_y=10\lambda$, $M=N=10$)

from the boundary edge between cover and guiding part increases because of the bigger magnitude of the field at the edge comparing to the case of $n_c=1.0$. Thus the radiation field increases and the wavelength characteristics becomes more asymmetry than the case of $n_c=1.0$.

Fig.6 shows the case where the refractive index of cover part is also changed periodically (n_{c1}, n_{c2}) similarly as the substrate part. It is confirmed that even in $n_c=3.0$ the radiation field R_r can be suppressed also by making the cover part periodic structure, that is, $n_{c1}=3.0$, $n_{c2}=2.88$ as shown in Fig.6.

Fig.7 shows the field distribution of the dominant guided mode and each discretized radiation mode. It is confirmed that each radiation field is negligibly small comparing to the dominant guided mode R^p_{g1} ($R^p_r/R^p_{g1}\leq 10^{-5}$), due to the suppression effect of the radiation field as investigated in this paper.

4. Conclusion

In the index-modulation type 3-D periodic waveguide with rectangular cross-section, the abnormal increase of reflected radiation field in the shorter wavelength region has been one of problems as a filter, and it has beenv difficult to obtain flattened wavelength characteristics in the main lobe of reflected dominant guided mode. In this paper, remarkable suppression of such a radiation field is achieved by making also the substrate part periodic structure similarly as guided part. Then, it is confirmed that, even in the index-modulation type 3-D embedded periodic waveguide with rectangular cross-section, the flattened wavelength characteristics can be obtained, and their behaviors are made clear.

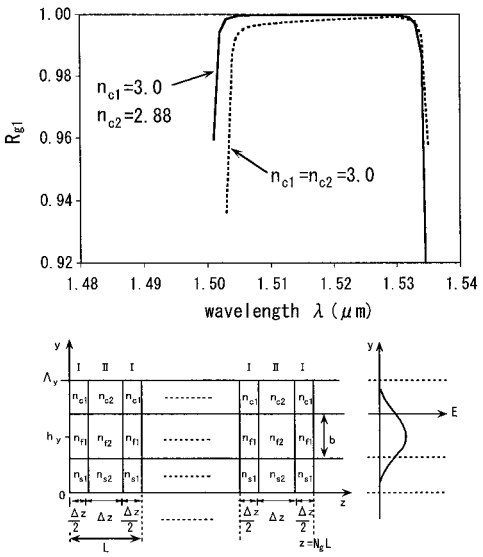

Fig.6 Wavelength characteristics of R_{g1} in improved index-modulation type periodic waveguide with $n_c=3.0$, when the cover part is also composed from periodic structure ($n_{c1}=3.0$, $n_{c2}=2.28$)
($n_{f1}=3.5$, $n_{f2}=3.38$, $n_{s1}=3.27$, $n_{s2}=3.15$, $2a=1.6[\mu m]$, $b=0.8[\mu m]$, $\Delta z=0.114[\mu m]$, $L=0.228[\mu m]$, $N_g=200$, $\Lambda_x=\Lambda_y=10\lambda$, $M=N=10$)

5. References

[1] M. Momoda, T. Miyamoto and K. Yasumoto, “Behavior of radiation field in shorter wavelength region in 3-dimensional periodic waveguide”, *Proc. of The* 2003 *IEICE Society Conf.*, C-1-13, p.13.

[2] T. Miyamoto, M. Momoda and K. Yasumoto, “Numerical analysis for three-dimensional optical waveguides with periodic structure using Fourier series expansion method”, *IEICE Trans. Electron.*, vol.J86-C, pp.591-600, June 2003 (in Japanese), *Electronics and Communication in Japan*, Part 2, vol.86, pp.22-31, Dec. 2003 (in English).

[3] M. Momoda, T. Miyamoto and K. Yasumoto, “Numerical analysis of lamellar grating type three-dimensional optical waveguide with periodic structure, using Fourier series expansion method”, *IEEJ Trans. FM,* vol.123, pp.1151-1158, Dec. 2003.

[4] M. Momoda, T. Miyamoto and K. Yasumoto, “Flattening of wavelength characteristics on reflected power of dominant guided mode in lamellar grating type periodic channel waveguide”, *Tech. Rep. IEICE*, OPE-2003-144, pp.7-12, Nov. 2003.

[5] M. Momoda, T. Miyamoto and K. Yasumoto, “Flattening of wavelength characteristics on dominant guided mode in lamellar grating type periodic channel waveguide”, *IEICE Trans. Electron* ., vol. J87-C, No.10, pp.784-785, Oct. 2004.

[6] A. Inoue, T. Iwashima, T. Enomoto, S. Ishikawa and H. Kanamori, “Optimization of fiber Bragg grating for dense WDM transmission system”, *IEICE Trans. Electron.*, vol.E-81-C, pp.1209-1218, Aug. 1998.

[7] M. Momoda, T. Miyamoto and K. Yasumoto, "Flattening of reflection characteristics of guided mode in index- modulation type periodic embedded optical waveguide with rectangular cross-section", *Proc. of The* 2004 *IEICE General Conf.*, C-3-17, p.190, Mar. 2004.

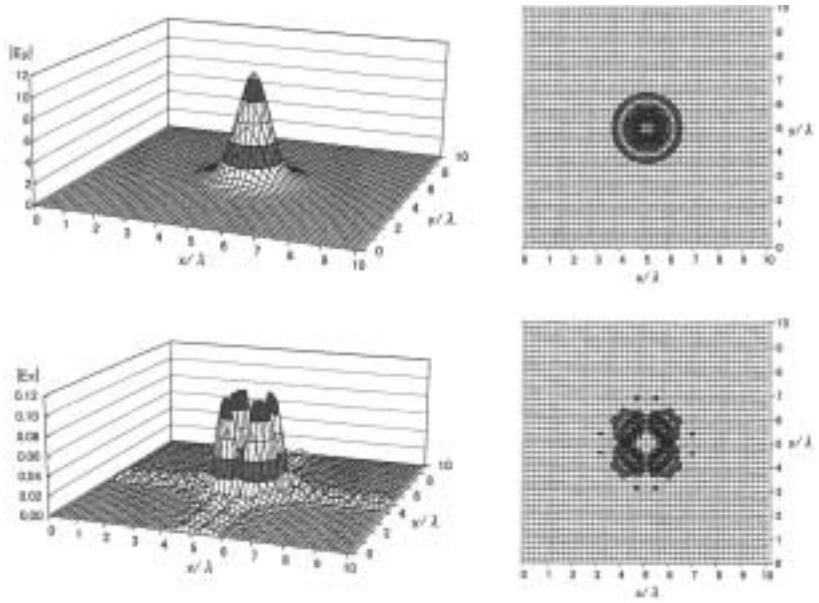

EH_{11} mode

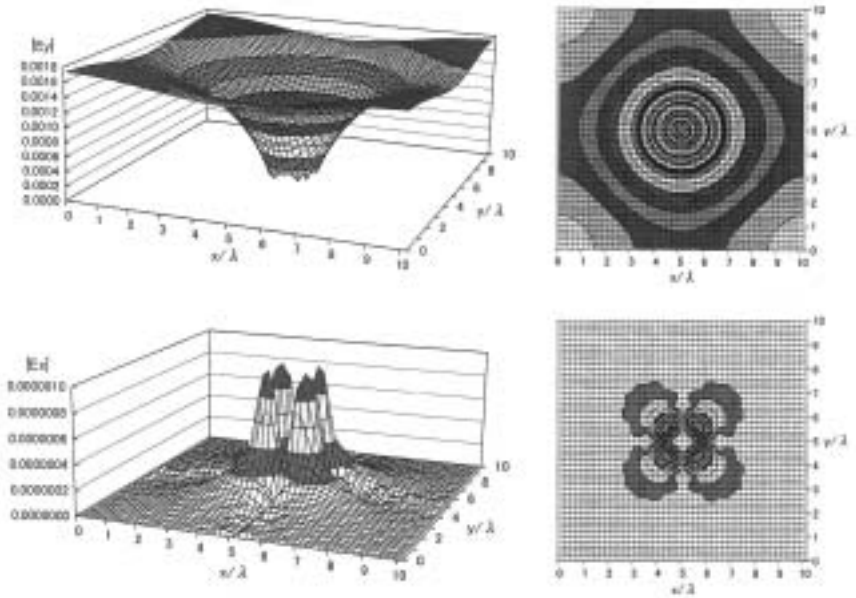

1st radiation mode (k=3)

7-(a)-1 Fiber Bragg grating (λ=1.465[μm], same parameters as Fig.1)

Fig.7 Field distribution

[8] M. Momoda, T. Miyamoto and K. Yasumoto, “Flattening of wavelength characteristics of reflected guided mode in index-modulation type periodic embedded optical waveguide with rectangular cross-section”, *Proc. of Asia Pacific Microwave Conf. APMC*'04, C8-1, pp.1-4, Dec. 2004.

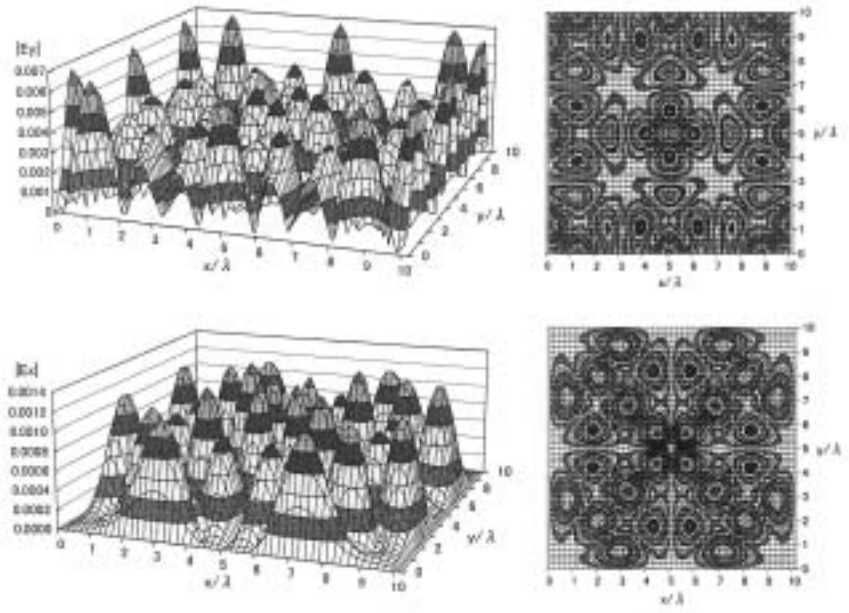

103th radiation mode (k＝105)

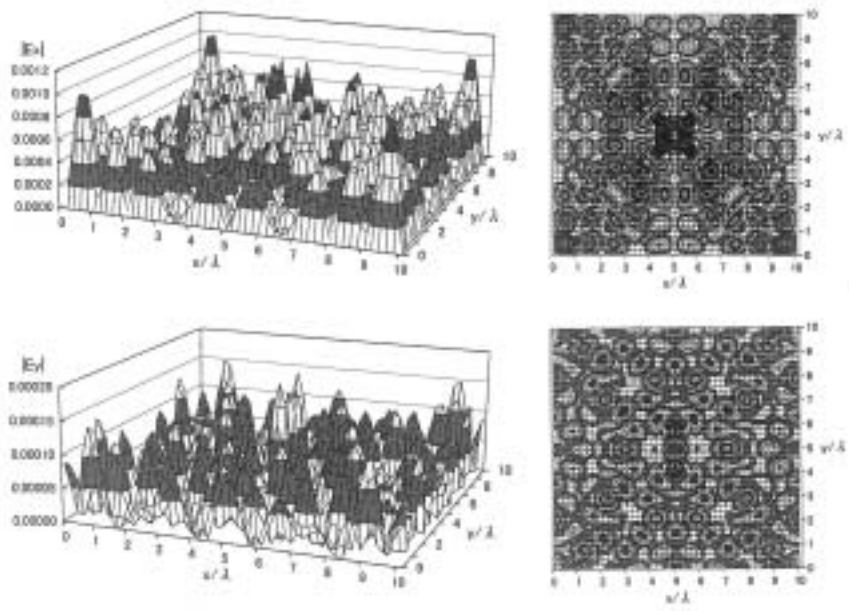

297th radiation mode (k＝299)

7-(a)-2

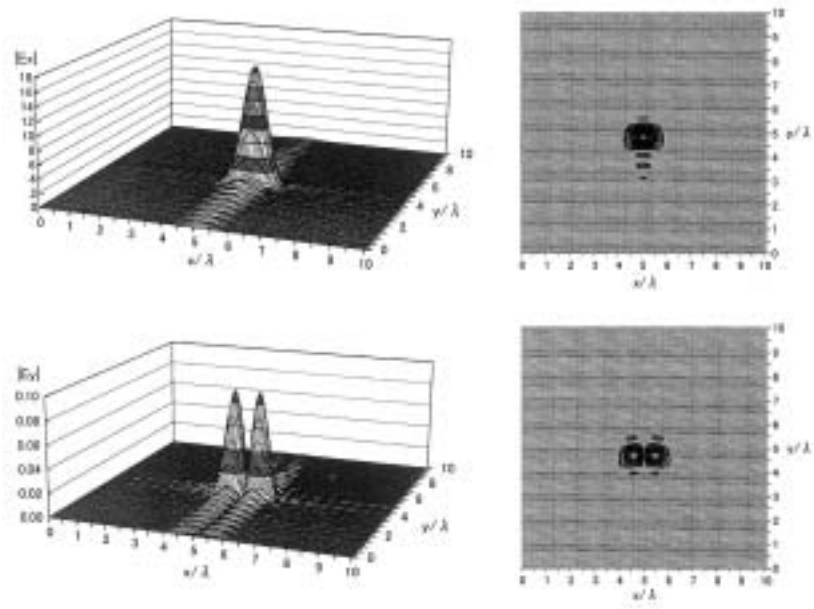

HE_{11} mode

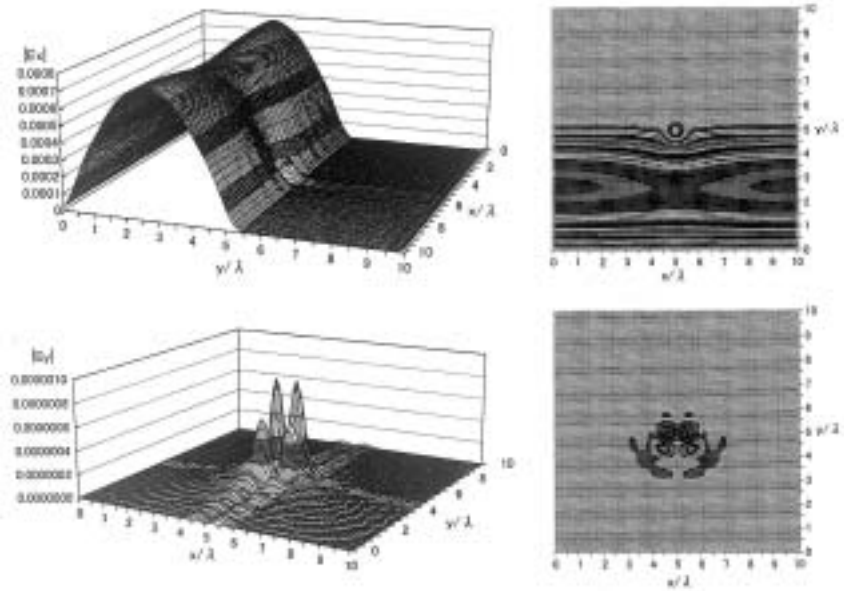

1st radiation mode (k=5)

7-(b)-1 Embedded 3-D periodic waveguide with air cover (λ=1.49[μm], same parameters as Fig.3)

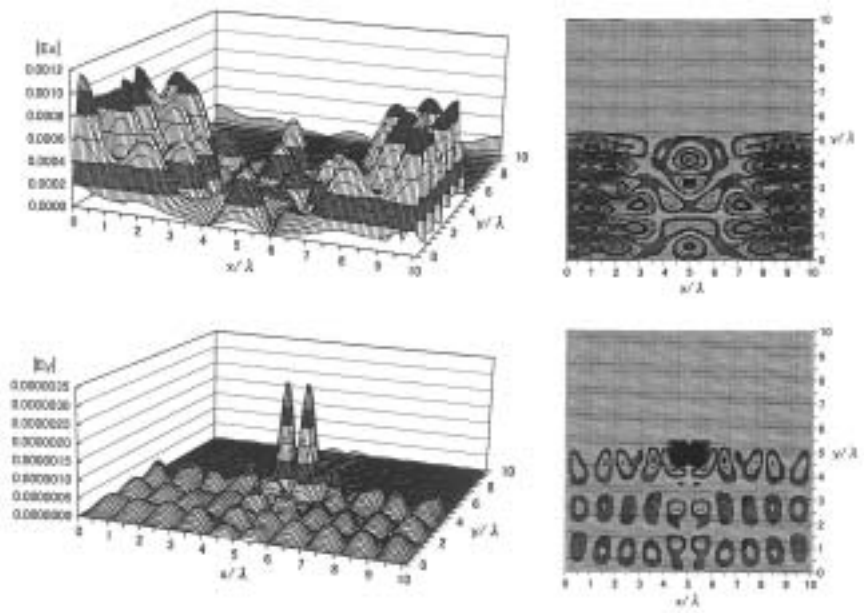

97th radiation mode (k＝101)

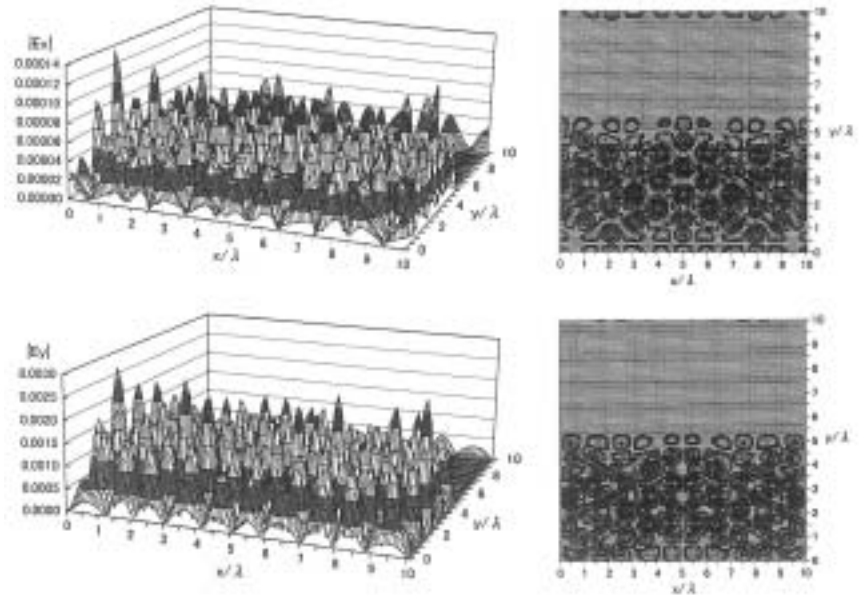

295th radiation mode (k＝301)

7-(b)-2